# Ion-Acoustic Density Hump Solitons in (r,q) Distributed Plasmas using Python

Muhammad Nouman Sarwar Qureshi[1]*, Ambar Tariq Sian[1], Laiba Emaan[1], Saba Khalid[1]
[1]Department of Physics, GC University, Lahore 54000, Pakistan
*Correspondence: noumansarwar@gcu.edu.pk

**Citation |** Qureshi. M. N. S, Sain. A. T, Emaan. L, Khalid. S, "Obliquely Propagating Nonlinear Electrostatic Waves with $(r,q)$ Distributed Electrons", IJIST Vol. 7 Issue. 1 pp 313-321, Feb 2025

**Received |** Jan 12, 2025 **Revised |** Feb 14, 2025 **Accepted |** Feb 16, 2025 **Published |** Feb 18, 2025.

Electron Velocity Distributions (EVDs) with a flat top at low energy and/or an enhanced tail at high energies are commonly observed in Earth's magnetosphere and solar wind. Noteworthy is the fact that only generalized $(r,q)$ distribution with two spectral indices fit such observed flat top distributions, since at low energies neither kappa nor Maxwellian distribution can fit the observed EVDs. In the limiting cases, $r=0, q\to\infty$ and $r=0, q=(\kappa+1)$; $(r,q)$ distribution reduces the Maxwellian and kappa distributions, respectively. In the current fluid model, for the first time, electrons are treated as $(r,q)$ distributed and Sagdeev potential is derived for fully nonlinear fluid equations for ion-acoustic waves and obtained density humps to interpret the observations. We analyzed the properties of solitary structures using observed plasma parameters and values of $r$ and $q$ indices that matched the reported values. We found that flat top distribution supports the density hump solitons with larger amplitude.

**Keywords:** Non-Maxwellian Distribution; $(r,q)$ Distribution; Electrostatic Solitary Waves; Solitons; Flat-Topped Distribution; Ion-Acoustic Waves

**Introduction:**

In the last couple of decades, many satellites have been sent to near-Earth space plasma orbiting the Earth on a 24/7 basis, which enables us to build distribution functions using these satellite data. A remarkable finding that emerged from such activity is; that distributions observed from different space plasma environments significantly deviate from the classical Maxwellian distribution due to the presence of flat tops and modified high-energy tails [1][2][3][4]. Until now, the Maxwellian velocity distribution was used to solve a wide variety of issues faced in many areas of space. Satellite data consistently show that particle velocity distributions in different regions of space deviate significantly from the Maxwellian distribution [5][6][7][8][9][10][11]. These frequent variations mean that the Maxwellian distribution is insufficient to comprehend or forecast various waves and instabilities. In the groundbreaking study conducted almost a decade ago, Qureshi et al. [12] constructed a new non-Maxwellian distribution that exhibits the flat top at lower energy and modified tails at higher energies. The distributions that are generally observed in space plasmas, ranging from flat-topped to kappa distributions, can be modelled using $(r,q)$ distribution. This characteristic established the (r,q) distribution as the most comprehensive and general distribution function.In plasma, ion-acoustic waves represent the fundamental wave mode where the magnetic field remains unchanged while the density undergoes compression. Linear theory successfully explains most of the wave events that occur in space plasmas. However, it is frequently insufficient and one must turn to nonlinear wave studies, which yield novel and significant insights and typically occur over vast spatial and temporal scale lengths. A defining feature of solitons is their ability to retain their shape after a collision, making them a distinctive nonlinear disturbance in the medium. Numerous disciplines, from solid-state to fluid dynamics, have realized the significance of the idea of solitons [13][14]. It has been conjectured that the Red Spot on Jupiter and the nerve impulse are solitons [15][16]. The discovery of ion-acoustic solitons was made experimentally using a double-plasma apparatus. Additionally, it has been assumed that they exist in the Earth's magnetosphere [17][18]. In the upper ionospheric auroral region, density humps associated with the ion-acoustic waves have been observed by Freja satellite [19][20]. Such nonlinear density structures are responsible for the acceleration of up-flowing ionospheric electrons and ions [21].

Therefore, in this paper, we studied the fully nonlinear ion-acoustic waves in a warm magnetized plasma and derive the Sagdeev potential for oblique propagation in a non-Maxwellian plasma where electrons are modelled by $(r,q)$ distribution. The central premise of this paper is the first-time application of the flat-top (r,q) electron distribution in a magnetized plasma to derive the density-hump structures observed by the Freja satellite. This phenomenon arises for the spectral indices $r$ and $q$, that corresponds to the flat-top at low energies and modified high energy tail, respectively.

**Model Equations:**

We consider a low-$\beta$ $\left(=\frac{8\pi n_o T_e}{B^2}\right)$ plasma, where charge quasineutrality and exact ion dynamics are assumed with electrons following $(r,q)$ distribution. The external magnetic field is oriented along the z-direction, $\boldsymbol{B}=B_0\boldsymbol{z}$, $\boldsymbol{E}=-\boldsymbol{\nabla}\varphi$ and propagation is considered in the $x\zeta$-plane given by $\boldsymbol{k}=k_x\hat{x}+k_z\hat{z}$ making an angle $\theta$ with the $\zeta$-axes. The governing fluid equations for such a plasma can be written in component form, as given below;

$$\frac{\partial n_i}{\partial t}+n_i\left(\frac{\partial v_x}{\partial x}+\frac{\partial v_z}{\partial z}\right)=0 \qquad (1)$$

$$\frac{\partial v_x}{\partial t}+\left(v_x\frac{\partial}{\partial x}+v_z\frac{\partial}{\partial z}\right)v_x=v_y-\frac{\partial\varphi}{\partial x}-\frac{\alpha}{n_i}\frac{\partial n_i}{\partial x} \qquad (2)$$

$$\frac{\partial v_y}{\partial t} + \left(v_x \frac{\partial}{\partial x} + v_z \frac{\partial}{\partial z}\right) v_y = -v_x \quad (3)$$

$$\frac{\partial v_z}{\partial t} + \left(v_x \frac{\partial}{\partial x} + v_z \frac{\partial}{\partial z}\right) v_z = -\frac{\partial \varphi}{\partial z} - \frac{\alpha}{n_i}\frac{\partial n_i}{\partial z} \quad (4)$$

In this paper, we employed a generalized $(r, q)$ distribution function to study the nonlinear ion-acoustic waves having the form [22]

$$f_{rq}(v) = \frac{3\,\Gamma[q]\,(q-1)^{-3/(2+2\,r)}}{4\,\pi\,c^{3/2}\,(2T_e/m_e)^{3/2}\,\Gamma\left[q-\frac{3}{2+2\,r}\right]\Gamma\left[1+\frac{3}{2+2\,r}\right]}\left[1+\frac{1}{q-1}\left(\frac{v^2-2e\phi/m_e}{c\,(2T_e/m_e)}\right)^{r+1}\right]^{-q} \quad (5)$$

where

$$c = \frac{3\,(q-1)^{-1/(1+r)}\,\Gamma\left[q-\frac{3}{2+2\,r}\right]\Gamma\left[\frac{3}{2+2\,r}\right]}{2\,\Gamma\left[q-\frac{5}{2+2\,r}\right]\Gamma\left[\frac{5}{2+2\,r}\right]} \quad (6)$$

where $\phi$ is the electrostatic potential, $T_e$ and $m_e$ are the electron temperature and mass respectively, $\Gamma$ is the gamma function, and $(2T_e/m_e)^{1/2}$ is the electron thermal velocity. The flat-top at lower energies and high energy tail can be modelled by spectral indices $r$ and $q$, respectively, which must satisfy conditions $q > 1$ and $q(r+1) > 5/2$.

Upon integrating Eq. (5) overall velocity space and assuming $\varphi \ll 1$, the total electron density can be written as [22]

$$n_e = 1 + A_{rq}\,\varphi \quad (7)$$

where $\varphi = e\phi/T_e$,

$$A_{rq} = \frac{\Gamma\left(\frac{1}{2(1+r)}\right)\Gamma\left(q-\frac{1}{2(1+r)}\right)}{2B\,\Gamma\left(\frac{3}{2(1+r)}\right)\Gamma\left(q-\frac{3}{2(1+r)}\right)} \quad (8)$$

and

$$B = \frac{\Gamma\left(\frac{3}{2(1+r)}\right)\Gamma\left(q-\frac{3}{2(1+r)}\right)}{3\Gamma\left(\frac{5}{2(1+r)}\right)\Gamma\left(q-\frac{5}{2(1+r)}\right)} \quad (9)$$

In the above set of Eqs. (1)-(5), $n_i$, $n_e$ are the ion and electron densities normalized by equilibrium density? $n_0$, $v_x, v_y,$ and $v_z$ are the $x$, $y$ and $z$-components of velocities normalized by $c_s\left(=\sqrt{\frac{T_e}{m_i}}\right)$, space coordinated by $\rho_i\left(=\frac{c_s}{\Omega_i}\right)$, time $t$ by $\Omega_i^{-1}$, where $e$ is the electronic charge, $\Omega_i = \frac{eB_O}{m_i}$ and $\alpha = \frac{T_i}{T_e}$.

**Derivation of Sagdeev Potential:**

In this study we introduced the commoving frame in normalized form as follows [23];

$$\eta = \frac{1}{M}(\sin\theta\ x + \cos\theta\ z - Mt) \quad (10)$$

where $M = \frac{v_p}{c_s}$ is known as the Mach number and $v_p = \frac{\omega}{k}$. Equations (1)-(4) then can be written, as

$$\frac{n_i}{M}\frac{d}{d\eta}(\sin\theta\, v_x + \cos\theta\, v_z) = \frac{dn_i}{d\eta} \quad (11)$$

$$(\sin\theta\, v_x + \cos\theta\, v_z - M)\frac{dv_x}{d\eta} = -\sin\theta\left(A_{rq} + \frac{\alpha}{n_i}\right)\frac{dn_i}{d\eta} + Mv_y \quad (12)$$

$$(\sin\theta\, v_x + \cos\theta\, v_z - M)\frac{dv_y}{d\eta} = -Mv_x \quad (13)$$

$$(\sin\theta\, v_x + \cos\theta\, v_z - M)\frac{dv_z}{d\eta} = -\cos\theta\left(A_{rq} + \frac{\alpha}{N}\right)\frac{dn_i}{d\eta} \qquad (14)$$

In the above set of Eqs. (11)-(14), we assumed the quasineutrality $n \approx n_i \approx n_e$, which is a valid approximation and can be used in low-frequency waves, such as ion-acoustic waves [9]. Upon integrating Eq. (11) for boundary conditions when $\eta \to \pm\infty, n_i \to 1, v_x = v_y = v_z = 0$, we obtained

$$\sin\theta\, v_x + \cos\theta\, v_z = (1 - 1/n_i)M \qquad (15)$$

Furthormore, we integrated Eqs. (12)-(14) using the boundary conditions $\eta \to \pm\infty, n_i \to 1, v_x = v_y = v_z = 0$. After solving, we obtained the three velocity components as: $v_x = \frac{1}{n_i}\frac{dv_y}{d\eta}$ (16)

$$v_y = \frac{1}{M\sin\theta}\left(A_{rq} + \frac{\alpha}{n_i} - \frac{M^2}{{n_i}^3}\right)\frac{dn_i}{d\eta} \qquad (17)$$

$$v_z = \frac{A_{rq}\cos\theta}{2M}({n_i}^2 - 1) + \frac{\alpha\cos\theta}{M}(n_i - 1) \qquad (18)$$

After putting Eq. (17) into Eq. (16) and then Eqs. (16) and (18) into Eq. (15), we get

$$\frac{1}{n_i}\frac{d}{d\eta}\left[\frac{1}{M}\left(A_{rq} + \frac{\alpha}{n_i} - \frac{M^2}{{n_i}^3}\right)\frac{dn_i}{d\eta}\right] = \left\{M\left(1 - \frac{1}{n_i}\right) + \frac{A_{rq}\cos^2\theta}{2M}(1 - {n_i}^2) + \frac{\alpha\cos^2\theta}{M}(1 - n_i)\right\} \qquad (19)$$

Now by multiplying terms in '[ ]' on both sides and simplifications, we get

$$\frac{1}{2}\frac{d}{d\eta}\left[\frac{1}{M}\left(R + \frac{\alpha}{n_i} - \frac{M^2}{{n_i}^3}\right)\frac{dn_i}{d\eta}\right]^2 = \left\{M(n_i - 1) + \frac{R\cos^2\theta}{2M}(n_i - {n_i}^3) + \frac{\alpha\cos^2\theta}{M}(n_i - {n_i}^2)\right\}\left[\frac{1}{M}\left(R + \frac{\alpha}{n_i} - \frac{M^2}{{n_i}^3}\right)\frac{dn_i}{d\eta}\right] \qquad (20)$$

Upon integrating Eq. (20) using the same boundary conditions, we obtained an equation that resembled the equation for a particle moving in a pseudopotential potential. $\left(\frac{dn_i}{d\eta}\right)^2 + S(n_i) = 0$ (21)

where

$$S(n_i) = -\frac{M^2}{\left[\left(A_{rq} + \frac{\alpha}{n_i} - \frac{M^2}{{n_i}^3}\right)\right]^2}\left[A_{rq}\cos^2\theta\left(\frac{1}{2n_i} + \frac{n_i}{2} - 1\right) + \frac{A_{rq}}{2}(n_i - 1)^2 + \frac{1}{M^2}\left\{\frac{{A_{rq}}^2\cos^2\theta}{8}(2{n_i}^2 - {n_i}^4 - 1) - \frac{{A_{rq}}^2\cos^2\theta\alpha^2}{8}(n_i - 1)^2 + M^4\left(\frac{1}{n_i} - \frac{1}{2{n_i}^2} - \frac{1}{2}\right)\right\} + \alpha\left\{\cos^2\theta\left(\frac{1}{n_i} - 1\right) + (n_i - 1) + 2A_{rq}\cos^2\theta\,({n_i}^2 - 1) + \frac{4\cos^3\theta}{8M^2}(4n_i - {n_i}^3) - (\cos^2\theta - 1)\log n_i\right\}\right] \qquad (22)$$

is the Sagdeev potential.

**Python-based Algorithm**

```
import numpy as np
import matplotlib.pyplot as plt
from scipy.fftpack import fft, ifft
```

```
# Define simulation parameters
L = 50.0  # Spatial domain length
N = 256   # Number of grid points
dx = L / N  # Grid spacing
dt = 0.01  # Time step
t_max = 10.0  # Maximum time
x = np.linspace(-L/2, L/2, N)
# Plasma parameters (r, q) distributed plasmas
r = 0.5  # Nonthermal parameter
q = 1.6  # Distribution index
phi_0 = 1.0  # Soliton amplitude
w = 5.0  # Soliton width
# Define initial soliton profile
def initial_condition(x, phi_0, w):
    return phi_0 * np.cosh(x / w) ** -2
phi = initial_condition(x, phi_0, w)
# Fourier wavenumbers
k = 2 * np.pi * np.fft.fftfreq(N, d=dx)
# KdV coefficients (A and B depend on plasma parameters)
A = 1.0  # Nonlinearity coefficient (function of r, q)
B = 0.1  # Dispersion coefficient (function of r, q)
# Time evolution using pseudo-spectral method
def kdv_step(phi, k, A, B, dt):
    phi_hat = fft(phi)
    dphi_hat = -1j * k * fft(0.5 * A * phi**2) - B * (1j * k)**3 * phi_hat
    return np.real(ifft(phi_hat + dt * dphi_hat))
# Time-stepping loop
time = 0.0
phi_list = [phi]
while time < t_max:
    phi = kdv_step(phi, k, A, B, dt)
    phi_list.append(phi)
    time += dt
# Plot results
plt.figure(figsize=(8, 6))
for i in range(0, len(phi_list), len(phi_list) // 5):
    plt.plot(x, phi_list[i], label=f'Time {i * dt:.2f}')
plt.xlabel('Position (x)')
plt.ylabel('Amplitude (ϕ)')
plt.title('Ion-Acoustic Soliton Evolution')
plt.legend()
plt.grid()
plt.show()
```

**Numerical Results:**

For a soliton solution to exist, the Sagdeev potential (Eq. (22)) needed to meet the following conditions.

$$S(n_i)|_{n_i=1} = 0, \quad S'(n_i)|_{n_i=1} = 0, \quad S''(n_i)|_{n_i=1} < 0$$
$$S(n_i)|_{n_i=n_{max}} = 0, \quad S'(n_i)|_{n_i=n_{max}} > 0 \tag{23}$$

When the Sagdeev potential (Eq. (22)) satisfied the above conditions, the following condition on the Mach number is obtained.

$$\cos^2\theta\sqrt{A_{rq}+\alpha} < M < \sqrt{A_{rq}+\alpha} \qquad (24)$$

When the above condition was satisfied on the Mach number, we obtained the Sagdeev potential that corresponds to the density hump soliton. We plotted the Sagdeev potential (Eq. (22)) for different values of spectral indices $r$, $q$ and Mach number satisfying the condition 924) and then plot the soliton structures which were obtained numerically from Eq. (22).

In Figure.-1(a), Sagdeev potential is depicted for different values of $r$ for fixed values of $q$, $M$ and $\theta$. We observed that Sagdeev potential's depth and width increase with the increasing value of $r$. Solitons corresponding to the Sagdeev potentials in Figure.-1(a) are plotted in Figure.-1(b). It can be noted that an increase in r makes the density hump structures taller and more slender. In Figure.-2(a) Sagdeev potential is depicted for different values of $q$ for fixed values of $r$, $M$ and $\theta$. It was observed that the depth and width of the Sagdeev potential increased with the rising value of $q$. Solitons corresponding to the Sagdeev potentials in Figure.-2(a) are plotted in Figure.-2(b). We also noted that an increase in $q$ makes the density of hum structures taller and slenderer. In Figure.-3(a) Sagdeev potential was depicted for different values of $M$ for fixed values of $r$, $q$ and $\theta$. It was observed that the depth and width of the Sagdeev potential increased with the rising Mach number $M$. Solitons corresponding to the Sagdeev potentials in Figure.-3(a) are plotted in Figure.-3(b). We observed that an increase in $M$ makes the density of hum structures taller and slenderer.

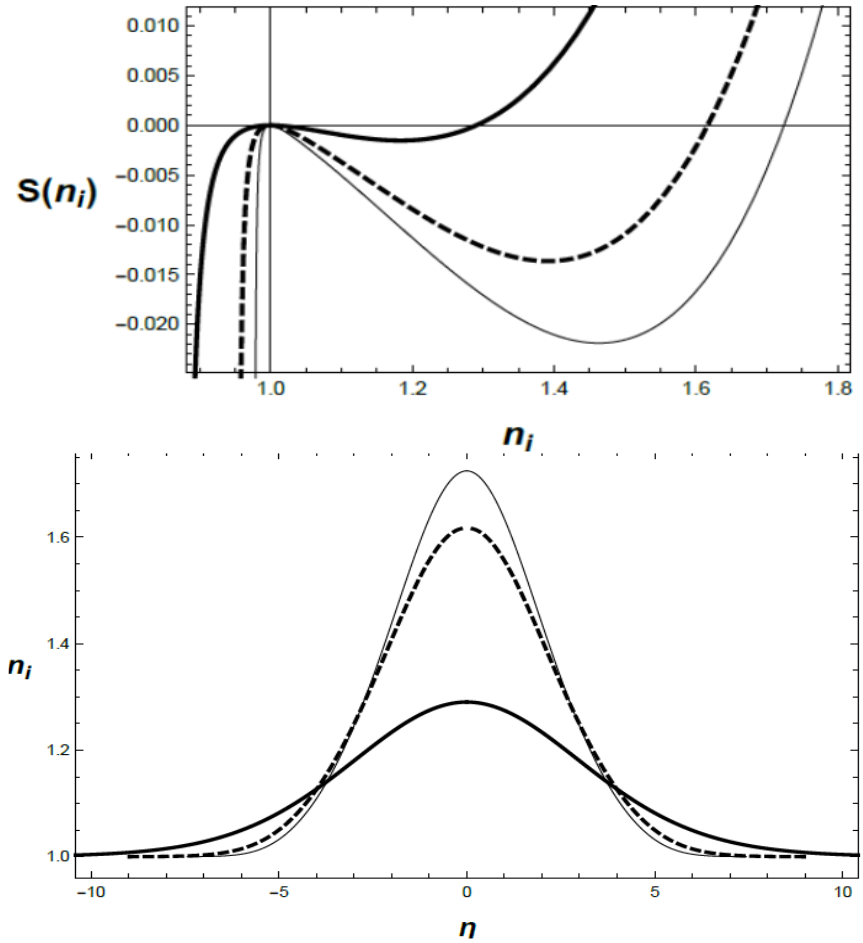


**Figure 1:** Sagdeev potential structures (upper panel) and corresponding solitons (lower panel) for different values of $r = 1$ (thick line), $r = 2$ (dashed line), $r = 3$ (thin line) when $q = 2$, $M = 0.85$, $\theta = 45^{\circ}$ and $\tau = 0.1$.

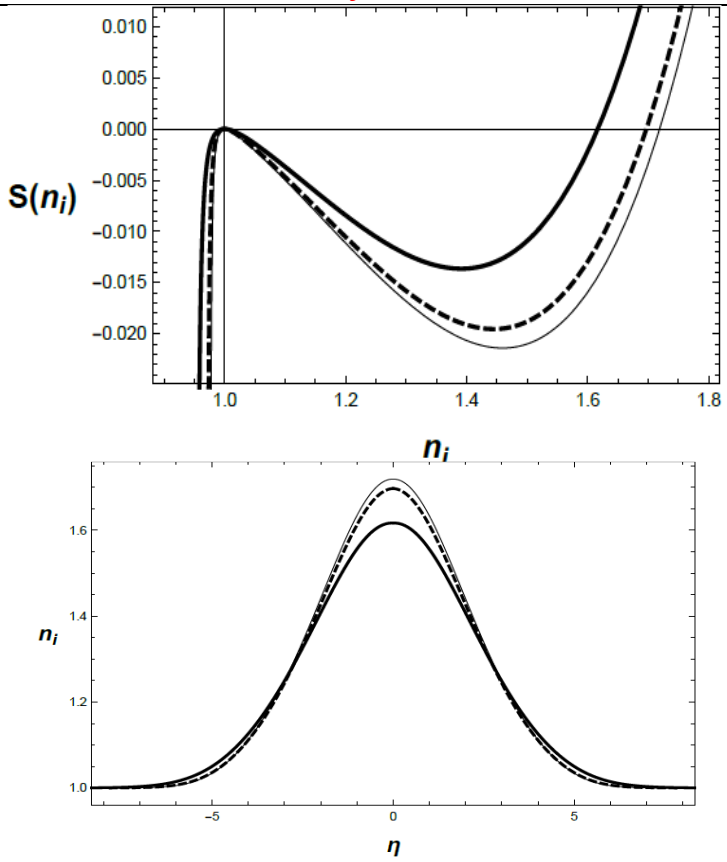


**Figure 2:** Sagdeev potential structures (upper panel) and corresponding solitons (lower panel) for different values of $q = 2$ (thick line), $q = 4$ (dashed line), $q = 7$ (thin line) when $r = 2$, $M = 0.85$, $\theta = 45^{\circ}$ and $\tau = 0.1$.

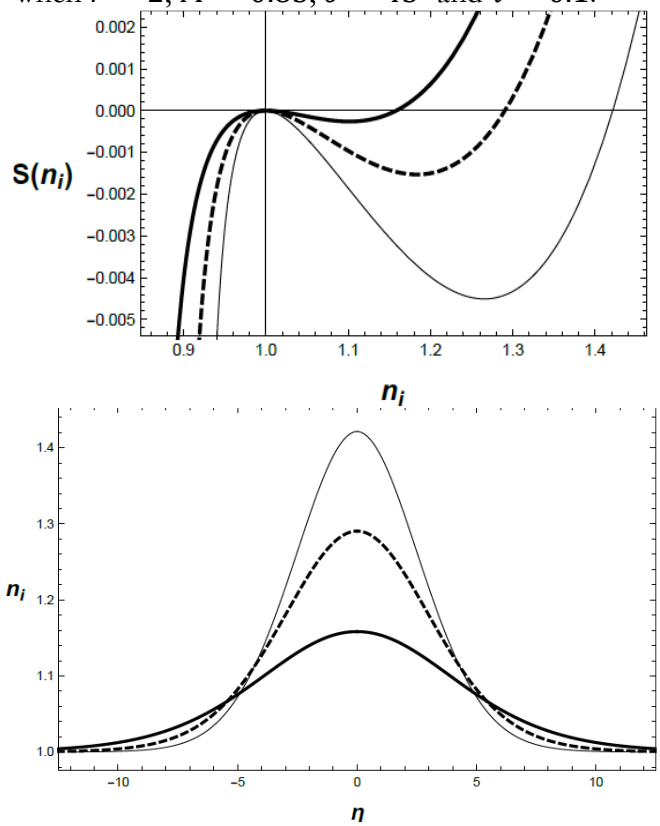

**Figure 3:** Sagdeev potential structures (upper panel) and corresponding solitons (lower panel) for different values of Mach number $M = 0.80$ (thick line), $M = 0.85$ (dashed line), $M = 0.90$ (thin line) when $r = 1, q = 2, \theta = 45^{\circ}$ and $\tau = 0.1$.

This paper presented a comprehensive nonlinear formulation in a warm, magnetized plasma for electrostatic waves such as ion-acoustic waves. To obtain the nonlinear wave solution, quasi-neutrality is taken into account in the fluid equations and assumed that electrons follow $(r, q)$ distribution. For the analysis of nonlinear ion-acoustic waves and their propagation characteristics, we used the pseudo-potential or Sagdeev potential technique and the Mach number range is derived under which solitary structures are obtained. Our model results showed that density hump solitons can be formed as observed by the Freja satellite in the upper ionospheric region. We found that if either of the spectral indices $r$ or $q$ increases, the soliton becomes taller and slenderer. As the value of $r$ increases, the distribution tends to exhibit a flat top and consequently, the number of low-energy particles increases. Also, as the value of $q$ increases, the distribution tends to exhibit a high-energy tail and consequently, the number of high-energy particles increases. Thus the flat top distribution with a high-energy tail supports the observations of density hump structures with larger amplitude and thinner profiles. Moreover, we found an increase in Mach number makes the soliton taller and slenderer. It has been observed that in the auroral region, density hump structures associated with the ion-acoustic waves have been observed by Freja and Viking satellites [19][20]. From the Figure. 1-3, we obtained the compressive solitary structures or density hump structures up to the order of 70% of the background value, which are in agreement with the observations of Freja and Viking satellites. Therefore, the results obtained in this study will explain the observations of density solitons in space plasmas where such non-Maxwellian distributions are observed.

**References:**


[1] N. M. B. A. A. Abid, M. S. Hussain, Amin Esmaeili, Abdullah Khan, S. Ali, M. Alharbi, Yas Al-Hadeethi, "Analyzing AZ-non-Maxwellian distributions in Earth's magnetosphere: MMS observations," *Sci. Rep.*, vol. 14, no. 29468, 2024, doi: https://doi.org/10.1038/s41598-024-74965-6.

[2] A. A. Abid, M. Z. Khan, Q. Lu, and S. L. Yap, "A generalized AZ-non-Maxwellian velocity distribution function for space plasmas," *Phys. Plasmas*, vol. 24, no. 3, Mar. 2017, doi: 10.1063/1.4977447/319371.

[3] M. S. Peiyun Shi, Prabhakar Srivastav, M. Hasan Barbhuiya, Paul A. Cassak, Earl E. Scime, "Laboratory Observations of Electron Heating and Non-Maxwellian Distributions at the Kinetic Scale during Electron-Only Magnetic Reconnection," *Phys. Rev. Lett.*, vol. 128, no. 025002, 2022, doi: https://doi.org/10.1103/PhysRevLett.128.025002.

[4] A. V. Daniel B. Graham, Yuri Khotyaintsev, M. André, "Non-Maxwellianity of Electron Distributions Near Earth's Magnetopause," *J. Geophys. Res. Sp. Phys.*, vol. 126, no. 10, 2021, doi: 10.1029/2021JA029260.

[5] D. J. G. Alexandros Chasapis, W. H. Matthaeus, T. N. Parashar, M. Wan, C. C. Haggerty, C. J. Pollock, B. L. Giles, W. R. Paterson, J. Dorelli, "In Situ Observation of Intermittent Dissipation at Kinetic Scales in the Earth's Magnetosheath," *Astrophys. J. Lett.*, vol. 856, no. 1, 2018, doi: 10.3847/2041-8213/aaadf8.

[6] H. Liang *et al.*, "Kinetic entropy-based measures of distribution function non-Maxwellianity: theory and simulations," *J. Plasma Phys.*, vol. 86, no. 5, p. 825860502, 2020, doi: 10.1017/S0022377820001270.

[7] A. N. F. W. Masood, S. J. Schwartz, M. Maksimovic, "Electron velocity distribution and lion roars in the magnetosheath," *ANGEO*, vol. 24, no. 6, pp. 1725–1735, 2006, doi: https://doi.org/10.5194/angeo-24-1725-2006.

[8] S. J. S. W. Masood, "Observations of the development of electron temperature anisotropies in Earth's magnetosheath," *Gen. Geophys. Res.*, 2008, doi:

https://doi.org/10.1029/2007JA012715.
[9] H. A. S. W. Masood, M. N. S. Qureshi, P. H. Yoon, "Nonlinear kinetic Alfvén waves with non-Maxwellian electron population in space plasmas," *JGR Sp. Physic*, 2015, doi: https://doi.org/10.1002/2014JA020459.
[10] S. J. S. M. N. S. Qureshi, Warda Nasir, W. Masood, P. H. Yoon, H. A. Shah, "Terrestrial lion roars and non-Maxwellian distribution," *JGR Sp. Physic*, 2014, doi: https://doi.org/10.1002/2014JA020476.
[11] L. A. A. S. Perri, D. Perrone, E. Yordanova, L. Sorriso-Valvo, W. R. Paterson, D. J. Gershman, B. L. Giles, C. J. Pollock, J. C. Dorelli, "On the deviation from Maxwellian of the ion velocity distribution functions in the turbulent magnetosheath," *J. Plasma Phys.*, vol. 86, no. 1, p. 905860108, 2020, doi: 10.1017/S0022377820000021.
[12] M. N. S. Q. H. A. S. G. M. S. J. S. F. Mahmood, "Parallel propagating electromagnetic modes with the generalized (r,q) distribution function," *Phys. Plasmas*, vol. 11, pp. 3819–3829, 2004, doi: https://doi.org/10.1063/1.1688329.
[13] M. A. H. Michelle D. Maiden, Dalton V. Anderson, Nevil A. Franco, Gennady A. El, "Solitonic Dispersive Hydrodynamics: Theory and Observation," *Phys. Rev. Lett*, vol. 120, no. 144101, 2018, doi: https://doi.org/10.1103/PhysRevLett.120.144101.
[14] H. E. Geeta Arora, Richa Rani, "Soliton: A dispersion-less solution with existence and its types," *Heliyon*, vol. 8, no. 5–6, p. e12122, 2022, doi: 10.1016/j.heliyon.2022.e12122.
[15] T. Maxworthy and L. G. Redekopp, "A solitary wave theory of the great red spot and other observed features in the Jovian atmosphere," *Icarus*, vol. 29, no. 2, pp. 261–271, Oct. 1976, doi: 10.1016/0019-1035(76)90054-3.
[16] H. C. Tuckwell, "Solitons in a Reaction-Diffusion System," *Science (80-. ).*, vol. 205, no. 4405, pp. 493–495, Aug. 1979, doi: 10.1126/SCIENCE.205.4405.493.
[17] H. Ikezi, R. J. Taylor, and D. R. Baker, "Formation and Interaction of Ion-Acoustic Solitions," *Phys. Rev. Lett.*, vol. 25, no. 1, p. 11, Jul. 1970, doi: 10.1103/PhysRevLett.25.11.
[18] H. Kikuchi, "Shocks, solitons and the plasmapause," *J. Atmos. Terr. Phys.*, vol. 38, no. 11, pp. 1055–1060, Nov. 1976, doi: 10.1016/0021-9169(76)90033-7.
[19] C. E. Seyler, "Lower hybrid wave phenomena associated with density depletions," *J. Geophys. Res. Sp. Phys.*, vol. 99, no. A10, pp. 19513–19525, Oct. 1994, doi: 10.1029/94JA01572.
[20] J. -E Wahlund *et al.*, "On ion acoustic turbulence and the nonlinear evolution of kinetic Alfvén waves in aurora," *Geophys. Res. Lett.*, vol. 21, no. 17, pp. 1831–1834, Aug. 1994, doi: 10.1029/94GL01289.
[21] R. P. C. W. Carlson, J. P. McFadden, R. E. Ergun, M. Temerin, W. Peria, F. S. Mozer, D. M. Klumpar, E. G. Shelley, W. K. Peterson, E. Moebius, R. Elphic, R. Strangeway, C. Cattell, "FAST observations in the downward auroral current region: Energetic upgoing electron beams, parallel potential drops, and ion heating," *Geophys. Res. Lett.*, 1998, doi: https://doi.org/10.1029/98GL00851.
[22] K. H. S. M. N. S. Q. W. M. H. A. Shah, "An alternative explanation for the density depletions observed by Freja and Viking satellites," *AIP Adv.*, vol. 8, no. 085010, 2018, doi: https://doi.org/10.1063/1.5040944.
[23] L. C. Lee and J. R. Kan, "Nonlinear ion-acoustic waves and solitons in a magnetized plasma," *Phys. Fluids*, vol. 24, no. 3, pp. 430–433, Mar. 1981, doi: 10.1063/1.863389.